J Appl Electrochem (2009) 39:1437–1442
DOI 10.1007/s10800-009-9820-7

ORIGINAL PAPER

Effect of a net on the limiting current distribution in a parallel plate electrochemical reactor. Part II: combined effects

Murali Venkatraman · J. W. Van Zee

Received: 9 October 2006 / Accepted: 29 January 2009 / Published online: 13 February 2009

Abstract In Part I, we used computational fluid dynamics (CFD) to solve the Navier-Stokes equations surrounding the inert net in a parallel plate channel and presented the individual effects of the transverse and longitudinal ribs on the limiting current density distribution. The type, location, spacing, and number of the ribs of the net were shown to affect the local and average current density distributions on each of the two electrodes. In Part II, we present the combined effects of the longitudinal and transverse ribs on the limiting current distribution. We calculated the enhancement factors for both the combined and individual effects and compared. The longitudinal ribs decreased the average current density whereas the transverse ribs increased the average current density relative to the no-net parallel plate reactor system. A maximum enhancement of 250% in the average current density for a spacing of 0.94×10^{-3} m was obtained with 16 transverse ribs. For the same spacing, a negative 70% enhancement was obtained with 14 longitudinal ribs and no transverse ribs. A maximum enhancement of 180% was observed for the entire net (14 longitudinal and 29 transverse ribs). The enhancements at each electrode are different for a given geometry.

Keywords Enhancement factor · Limiting current · Longitudinal and transverse ribs · Nusselt number distribution · Obstructed channel flow

M. Venkatraman (✉) · J. W. Van Zee
Department of Chemical Engineering, University of South Carolina, Columbia, SC 29208, USA
e-mail: Murali.Venkatraman@csiro.au

Present Address:
M. Venkatraman
CSIRO Materials Science and Engineering, Private Bag 33, Clayton South MDC, VIC 3169, Australia

List of symbols

h_1	Thickness of transverse rib in z direction (m)
h_2	Thickness of longitudinal rib in z direction (m)
i	Local current density (A m^{-2})
i_{avg}	Plate-average current density (A m^{-2})
$i_{avg\text{-}noribs}$	Plate-average current density for no-ribs case(A m^{-2})
i^*	Normalized local current density (dimensionless)
L	Electrode length in y direction (m)
W	Electrode width in x direction (m)
w_1	Width of the longitudinal rib in x direction (m)
w_2	Width of the transverse rib in y direction (m)

Greek symbols

Δ	Deviation factor (dimensionless)
η	Non-dimensional x coordinate
ζ	Non-dimensional y coordinate
λ	Enhancement factor [dimensionless Equation (1)]

Subscripts

1	Electrode 1
2	Electrode 2
avg	Average
avg_noribs	Average for the no-ribs case

Superscripts

*	Dimensionless quantity obtained by dividing respective quantity by its average

1 Introduction

In Part I [1], our CFD study predicted the individual effects of the longitudinal and transverse ribs as a function of the number, position and spacing of the ribs. A non-dimensional

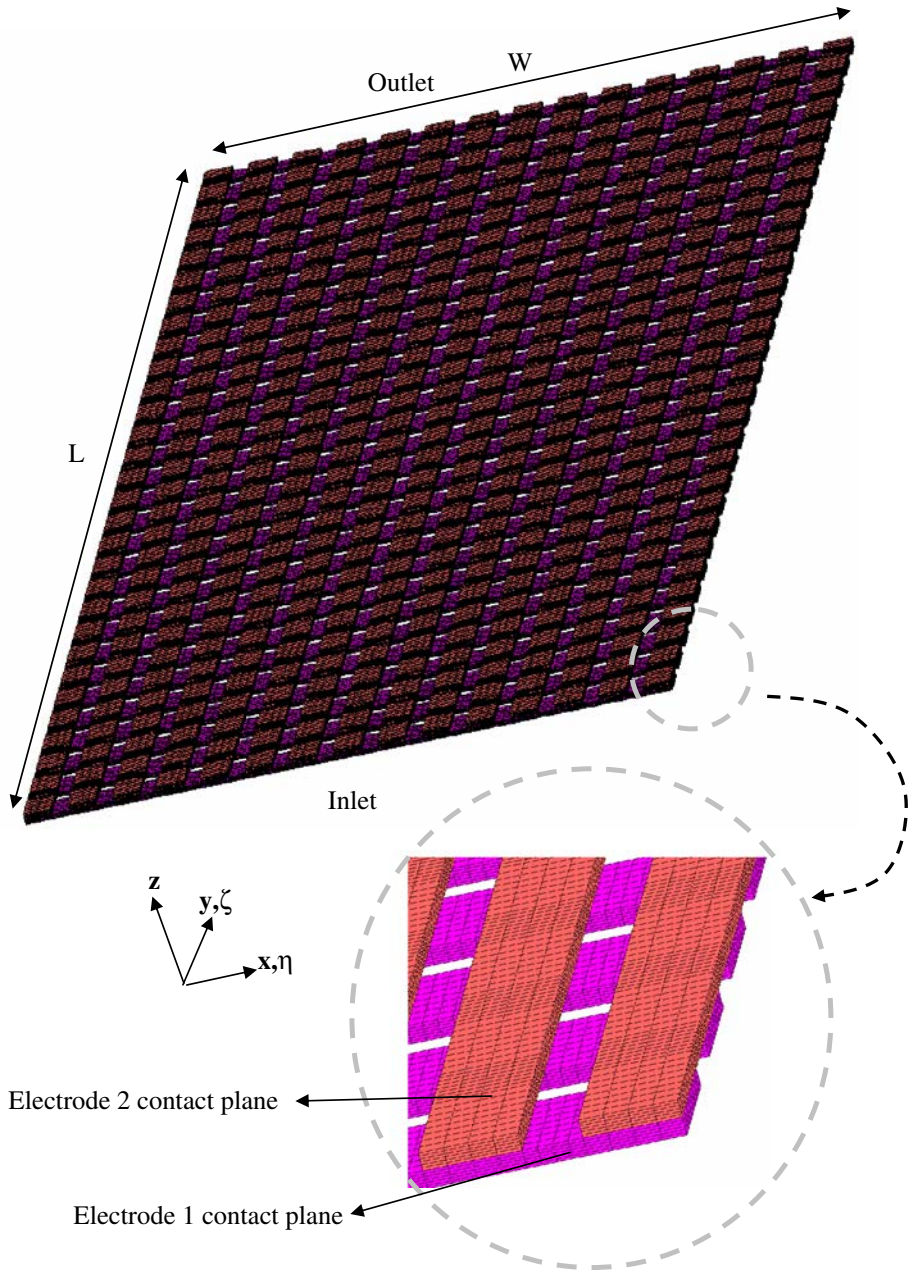

Fig. 1 Schematic of a typical computational mesh (exploded view in the encircled figure). Note that a maximum of equally spaced 14 longitudinal and 29 transverse ribs were used in the study. The computational mesh shows the fluid domain and not the net with the ribs which is situated in the space between the computational cells

current density (i^*) and a deviation factor (Δ) were introduced to quantify the effect of the ribs on the limiting current distribution of the two electrodes (refer Equations (11) and (15), Part I [1]). It was shown that the transverse ribs affected the limiting current density distribution more significant than the longitudinal ribs. With longitudinal ribs the effect of the number of ribs was more significant than the position and spacing between the ribs. However, with transverse ribs, the position, number, and spacing between the ribs were found to significantly affect the limiting current distribution. Here, we extend the work to the combined effects of the longitudinal and transverse ribs and calculate the enhancements in current density obtained at both electrodes for both the individual and combined effects.

2 Mathematical model

The details of the geometry and the boundary conditions can be found in Part I [1]. Figure 1 shows a typical computational mesh used in this study. The mesh shows only the domain where the fluid flows (which has a net-like structure) and not the net itself. The net is located in the space between the computational cells. No-slip conditions at all

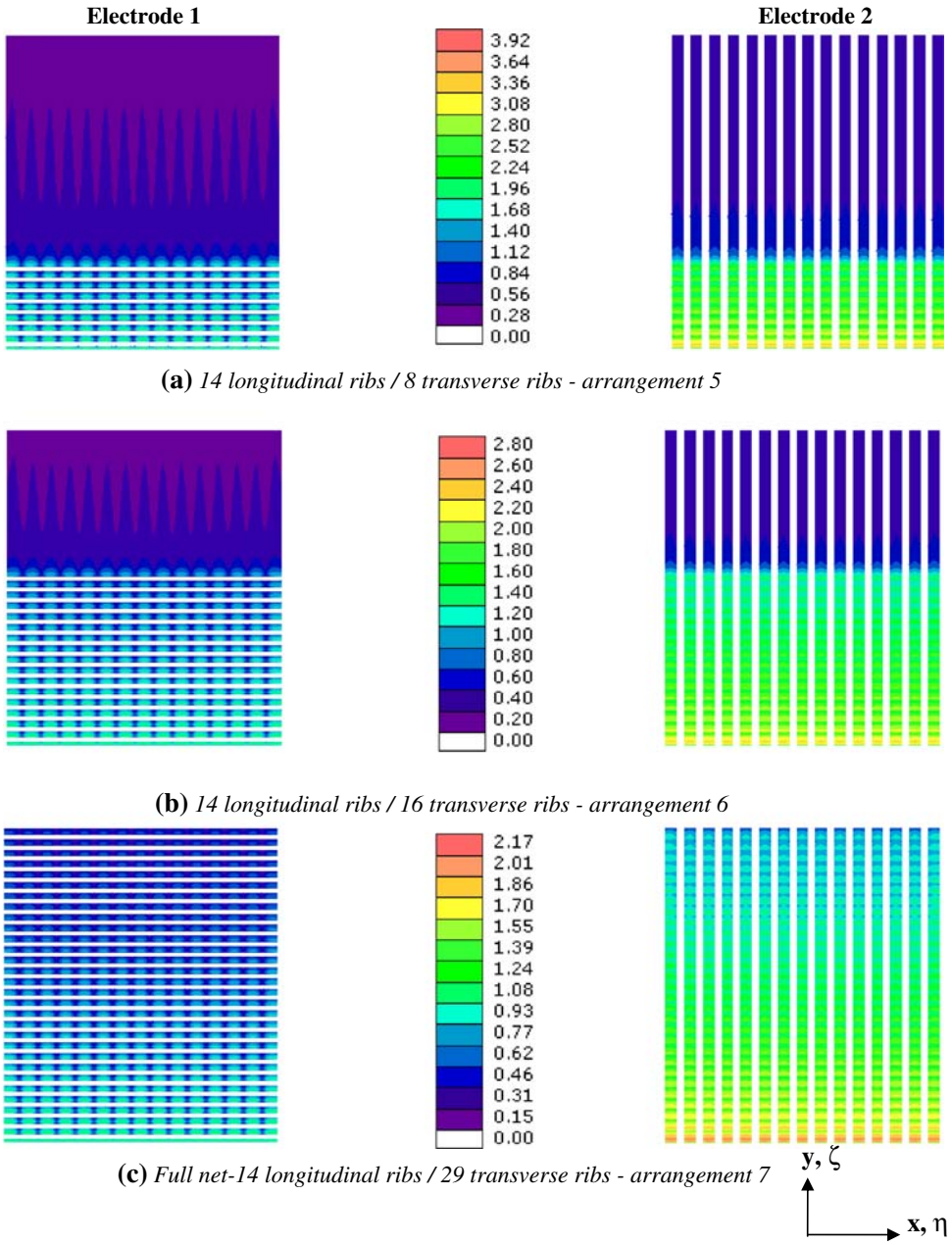

(a) *14 longitudinal ribs / 8 transverse ribs - arrangement 5*

(b) *14 longitudinal ribs / 16 transverse ribs - arrangement 6*

(c) *Full net-14 longitudinal ribs / 29 transverse ribs - arrangement 7*

Fig. 2 Distribution of the normalized local current density i^* for the case for 8, 16, and 29 transverse ribs with 14 longitudinal ribs. The spacing between the transverse ribs is maintained at $(l_2/L) = 0.0214$. The spacing between longitudinal ribs is maintained at $(l_2/L) = 0.0214$. Refer to Table 1 (Part I) for dimensions

the fluid-solid interfaces are assumed. The electrolyte fluid enters through a diffuser (not shown) at a constant velocity 0.01 m s^{-1}, and the free stream velocity is well established prior to contacting the inert net. The current density (i) is calculated based on a centerline concentration and is non-dimensionalized (i^*) by dividing it with the corresponding average plate current density (i_{avg}) which is calculated based on the available plate area (Equation (11), Part I [1]).

3 Results and discussion

As in Part I [1], all the longitudinal ribs are taken to be of the same size. The transverse ribs are the same size, although they differ from the dimensions of the longitudinal ribs (Table 1, Part I [1]). The full net is formed by 29 transverse and 14 longitudinal ribs.

Figure 2 shows three arrangements of 8, 16, and 29 transverse ribs with 14 longitudinal ribs. The arrangements are numbered sequentially starting with Part I for convenience. A representative section of this complex flow field is shown in Fig. 3. The combined effect of both types of ribs produces a complex flow field and the local current density follows the changes in the local velocity profile. The parabolic-like oscillations in the local current density distribution in the η direction, caused by the longitudinal ribs, are damped as more transverse ribs are added. Thus, transverse ribs produce a "dispersion" in the η direction.

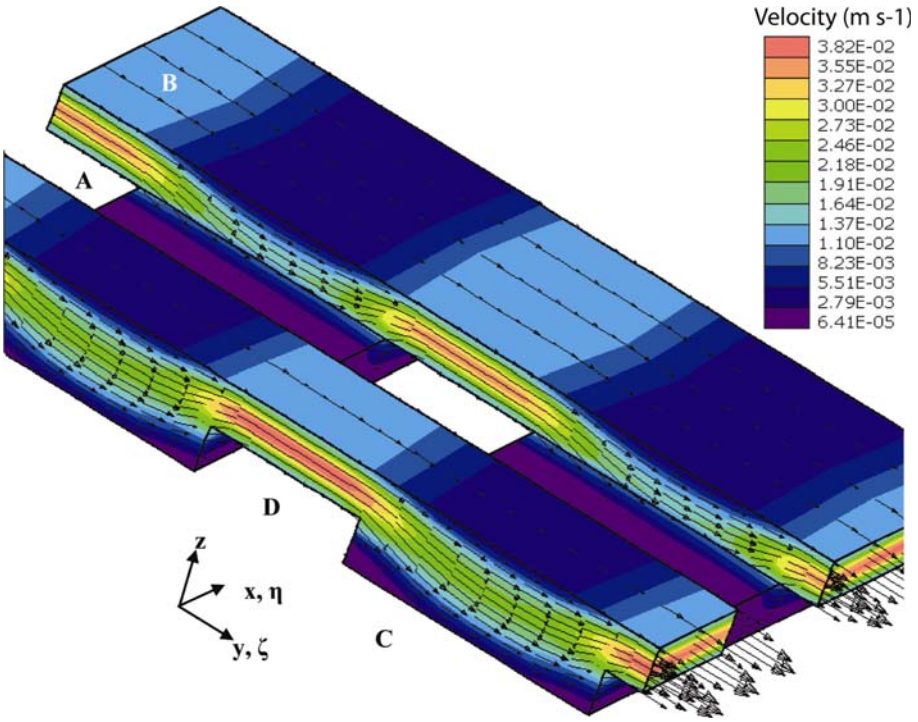

Fig. 3 A section of the flow field distribution for the net geometry shown in Fig. 2c. The flow inside the live cell spacing has been featured. The regions A, B, C, and D from Figs 5 and 9 of Part 1 have been featured to facilitate comparison

The overall effect of the ribs on the average current density can be quantified by an enhancement factor, λ, defined for a particular geometry and a particular electrode :

$$\lambda = \left(\frac{i_{avg}}{i_{avg-noribs}}\right)\left(\frac{A}{A_{noribs}}\right) \quad (1)$$

It may seem that the quantity $\left(\frac{i_{avg}}{i_{avg-noribs}}\right)$ in Eq. 1 could be interpreted as the enhancement of current density in the ribbed cases against the no-ribs case. However, the quantities i_{avg} and i_{avg_noribs} are calculated based on two different areas, A and A_{noribs}, respectively. A varies significantly with the number of ribs present. (Equations (6) and (7), in Part I [1]). Hence, a more consistent definition for enhancement factor would be based on the geometrical plate area A_{noribs} as given in Eq. 1. The variation of λ as a function of the number of longitudinal ribs (n_l) and number of transverse ribs (n_t) is given in Figs. 4 and 5 respectively.

Figure 4 shows that the longitudinal ribs produce negative enhancement (i.e. $\lambda < 1$) at both the electrodes. The decrease in λ at electrode 1 is negligible. The decrease in λ is more significant in the case of electrode 2 to which the longitudinal ribs are attached and is primarily due to the decrease in the ratio of areas $\left(\frac{A}{A_{noribs}}\right)$ in Eq. 1. The values of $\left(\frac{i_{avg}}{i_{avg-noribs}}\right)$ for various cases of longitudinal ribs were close to 1.0, showing that the effect of longitudinal ribs is similar to dividing the channel into smaller parallel subchannels without a loss or gain in average current density. However, in the limiting case where the longitudinal ribs would block the entire plate area of the electrode 2, the enhancement must be zero, since the current density is zero all over. This limiting case however, is not predicted if $\left(\frac{i_{avg}}{i_{avg-noribs}}\right)$ is used as the enhancement factor. This further emphasizes that the ratio of areas $\left(\frac{A}{A_{noribs}}\right)$ needs to be included in the calculation of a more realistic enhancement in Eq. 1.

However, in the case of transverse ribs the variation of enhancement factor shows a different behavior. Figure 5 shows that, initially λ increases with increase in the number of transverse ribs for both electrodes. However, λ attains a maximum at 16 transverse ribs and decreases thereafter for both electrodes. Initially when the transverse ribs are added to electrode 1, it creates regions **C** and **D** (Fig. 3)**.** Region **D** has a much higher average velocity than the no-ribs case Whereas the average velocity of region **C**, is comparable to the no-ribs case. Hence, initially the average current density and the ratio $\left(\frac{i_{avg}}{i_{avg-noribs}}\right)$ increase. However, as more transverse ribs are added, the ratio $\left(\frac{A}{A_{noribs}}\right)$ decreases considerably and λ attains a maximum at 16 ribs [roughly half of the total number of transverse ribs (29) in the full net]. Beyond that, λ decreases with any further addition of transverse ribs. This decrease is also consistent with λ approaching zero in the limiting case of transverse ribs blocking the entire plate area of electrode 1. The work of Venkatraman [2] suggests that λ would be different if the position and spacing of the transverse ribs are altered, but that is reserved for future work. Therefore, in this paper, all the configurations of transverse ribs studied for the

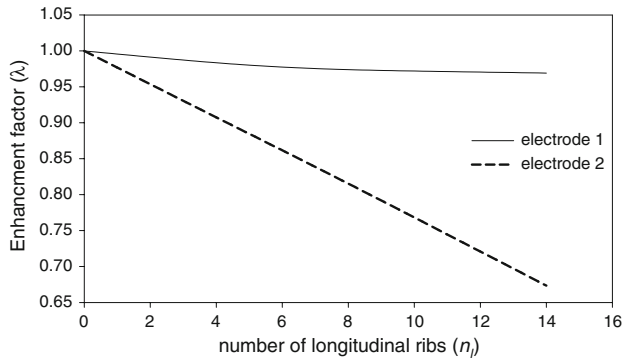

Fig. 4 Variation of the enhancement factor λ, as a function of number of longitudinal ribs n_l only

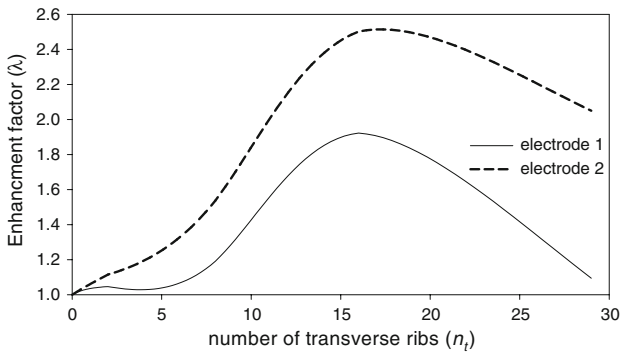

Fig. 5 Variation of the enhancement factor λ, as a function of number of transverse ribs n_t only

calculation of enhancement factor, feature equal spacing between successive ribs where the spacing is equal to l_2 (Table 1, Part I). Figure 2 shows some of these configurations. The longitudinal ribs do not show a similar effect and the enhancement is unaffected by the positioning and spacing of the longitudinal ribs. In addition, it for the same number of ribs, the negative enhancement produced by the longitudinal ribs is much less than the positive enhancement produced by the transverse ribs.

Figure 6 shows the combined effect of longitudinal and transverse ribs on the variation of the enhancement factor for 14 longitudinal ribs and multiple transverse ribs. The behavior of both electrodes is consistent with the explanations presented for Figs. 4 and 5. Electrode 1 shows a maximum plateau although a decrease beyond 16 transverse ribs is not observed unlike Fig. 5. On the other hand, electrode 2 does not show a plateau although the rate of increase in enhancement decreases beyond 16 transverse ribs. In addition the graph for electrode 2 starts at 0.67 and not at 1.0. The lower value 0.67 corresponds to the negative enhancement produced by the 14 longitudinal ribs which would be 1.0 if no longitudinal ribs were present. The transverse ribs clearly increase the enhancement although from a lower value. At high Reynolds numbers and considerable rib heights (i.e. h_1 and h_2, Fig. 1, Part I [1]) turbulence and recirculation may occur at different parts of the channel. In such cases, the dependency of λ on the number and type of ribs may be considerably different from what is displayed in the present system. Thus for the system and conditions presented in this paper, it could be concluded that, in order to enhance the mass transfer characteristics the number of longitudinal ribs must be kept as low as the structural requirements allow. Transverse ribs could be added to enhance, but too many beyond a certain number could produce negative enhancement as shown in Fig. 5. Keeping the number of ribs low and allowing more spacing between successive ribs increases the enhancement factor. An optimal number of ribs, properly spaced, which would ensure structural integrity and good mass transfer, is sought for the design of SFC and is the topic of future work.

4 Conclusions

A numerical study of the effect of the net geometry on the limiting current density distribution in a parallel plate channel was presented. The net geometry affects the parabolic velocity profiles significantly, resulting in zones of high, low, and zero mass transfer. The type, positioning, spacing and number of ribs have a significant effect on the fluid flow and current density distribution. Current density was found to follow the velocity profiles. The results show that the longitudinal ribs decrease the average current density whereas the transverse ribs increase the average current density relative to the no-net parallel plate channel. The behavior of the ribbed systems was presented as enhancement in the average current density of the no-ribs case. The dependence of enhancement in average current density on the number of longitudinal and transverse ribs was presented. The effect of transverse ribs on the current distribution was found to be drastic and much higher than

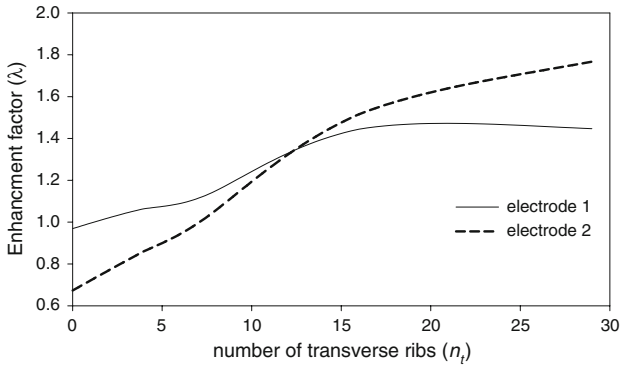

Fig. 6 Combined effect of longitudinal and transverse ribs: variation of the enhancement factor λ, as a function of number of transverse ribs n_t. for a given 14 longitudinal ribs

the longitudinal ribs. A maximum enhancement of 250% in the average current density for a spacing of 0.94×10^{-3} m was obtained with 16 transverse ribs. For the same spacing, a negative 70% enhancement was obtained with 14 longitudinal ribs and no transverse ribs. A maximum enhancement of 180% was observed for the entire net (14 longitudinal and 29 transverse ribs). The enhancements at each electrode were different for a given geometry. The enhancement factor could be used as a design tool for the net-based parallel plate reactor systems. The numerical results have a less than 5% error for the no-ribs case except at the entrance of the channel and at the transverse ribs where the error is around 8%.

Acknowledgement The authors acknowledge Dr. Sirivatch Shimpalee of University of South Carolina, for his useful inputs in the CFD calculations.

References

1. Venkatraman M, Van Zee JW (2009) Effect of a net on the limiting current distribution in a parallel plate electrochemical reactor: part I. individual effects. J. Appl. Electrochem. doi:10.1007/s10800-009-9819-0
2. Venkatraman M (2006) Models for mass transfer effects in semi-fuel cells and for a Silver–Zinc battery. Dissertation, University of South Carolina, Columbia